

In-situ investigation of melting characteristics of waste selective catalytic reduction catalysts during harmless melting treatment*

Hao ZHOU^{†1,2}, Yu-jian XING^{1,2}, Jia-nuo XU^{1,2}, Ming-xi ZHOU^{1,2}

¹State Key Laboratory of Clean Energy Utilization, Zhejiang University, Hangzhou 310027, China

²Institute for Thermal Power Engineering, Zhejiang University, Hangzhou 310027, China

[†]E-mail: zhouhao@zju.edu.cn

Received June 10, 2020; Revision accepted July 17, 2020; Crosschecked Jan. 14, 2021

Abstract: Selective catalytic reduction (SCR) catalyst waste is a hazardous solid waste that seriously threatens the environment and public health. In this study, a thermal melting technology is proposed for the treatment of waste SCR catalysts. The melting characteristics and mineral phase transformation of waste SCR catalysts blended with three different groups of additives were explored by heating stage microscopy, thermogravimetric analysis/differential scanning calorimetry (TG/DSC) analysis, thermodynamic simulation, and X-ray diffraction (XRD) analysis; heavy metal leaching toxicity was tested by inductively coupled plasma-atomic emission spectrometry (ICP-AES) analysis. The results indicated that the melting point of waste SCR catalysts can be effectively reduced with proper additives. The additive formula of 39.00% Fe₂O₃ (in weight), 6.50% CaO, 3.30% SiO₂, and 1.20% Al₂O₃ achieves the optimal fluxing behavior, significantly decreasing the initial melting temperature from 1223 °C to 1169 °C. Furthermore, the whole heating process of waste SCR catalysts can be divided into three stages: the solid reaction stage, the sintering stage, and the primary melting stage. The leaching concentrations of V, As, Pb, and Se are significantly reduced, from 10.64, 1.054, 0.195, and 0.347 mg/L to 0.178, 0.025, 0.048, and 0.003 mg/L, respectively, much lower than the standard limits after melting treatment, showing the strong immobilization capacity of optimal additives for heavy metals in waste SCR catalysts. The results demonstrate the feasibility of harmless melting treatments for waste SCR catalysts with relatively low energy consumption, providing theoretical support for a novel method of disposing of hazardous waste SCR catalysts.

Key words: Waste selective catalytic reduction (SCR) catalyst; Thermal melting treatment; Melting characteristics; Additives; Heating stage microscope; Leaching toxicity
<https://doi.org/10.1631/jzus.A2000192>

CLC number: X773

1 Introduction

Selective catalytic reduction (SCR) is a mainstream technology for eliminating hazardous NO_x emissions at coal-fired power plants. As a post-combustion NO_x control process, it shows high NO_x reduction efficiency through the reaction between ammonia and NO_x under the action of SCR catalysts.

The efficiency of the SCR process strongly depends on the activity of the SCR catalyst (You et al., 2012). However, owing to the coking of dust, ammonia salt, or the deposition, poisoning, and sintering of alkali metals, these catalysts have the drawback of deactivation after being used for several years (Zheng et al., 2005; Peng et al., 2015; Li et al., 2018). According to some researchers, the deactivated catalyst can recover its activity through regeneration treatment technology (Shang et al., 2012; Lee et al., 2013). Nevertheless, the number of regeneration times is limited, and so it will eventually end up as a waste catalyst.

Toxic substances such as V, Mo, As, Pd, and Se contained in waste SCR catalysts seriously harm

* Project supported by the National Key Research and Development Program of China (No. 2018YFB0604104)

 ORCID: Hao ZHOU, <https://orcid.org/0000-0001-9779-7703>;
Yu-jian XING, <https://orcid.org/0000-0002-1170-3516>

© Zhejiang University Press 2021

human health and the environment. In China, the vanadium-titanium-based waste SCR catalyst was incorporated into hazardous solid waste in 2014 and clearly classified as an HW50 waste catalyst in the national hazardous waste list (Chen et al., 2016). In addition, with the full implementation of ultra-low emission policies in China, the annual yield of waste SCR catalysts is sure to be enormous in the coming future, and consequently, the harmless treatment of waste SCR catalysts is an important issue in SCR denitration technology.

To date, there are two main treatment methods for waste SCR catalysts: landfill and metal recovery (Zhao et al., 2015; Wu et al., 2016; Choi et al., 2018). Unfortunately, the landfill method requires significant land resources, and the heavy metals existing in waste catalysts may escape into the environment in the long term. Valuable metals contained in waste SCR catalysts, such as V and W, can be recycled effectively by metal recovery; however, high operating costs limit industrial-scale application. As an alternative to the two methods described above, there is increasing interest in thermal treatment for solid waste. The thermal treatment process is now widely applied to industrial hazardous waste, in cases such as municipal solid waste incinerators (MSWIs), fly ash, or sewage sludge (Sakai and Hiraoka, 2000; Rani et al., 2008; Lindberg et al., 2015), and is considered a promising solution because of its significant advantages in weight and volume reduction, the digestion of inorganic pollutants, the solidification of heavy metals, and the resource utilization. Co-processing in cement kilns has been a well-developed waste treatment technology because of the advantages of high temperature, long residence times, and surplus oxygen (Kikuchi, 2001; Pan et al., 2008; Verbinnen et al., 2017). Numerous studies (Liu et al., 2015; Wang et al., 2016; Xiao et al., 2018) have proved that solid waste co-processing in cement kilns realizes resource utilization during the treatment of hazardous solid waste, and controls the emission of heavy metal and dioxin contaminants, keeping them within an acceptable level by a series of operations, such as accelerated carbonation and water-washing pretreatment. Furthermore, co-processing by iron ore sintering is also a promising method for the harmless treatment of hazardous waste, which achieves safe disposal and maintains the sintering strength and yield (Min et al.,

2017, 2018; Xu et al., 2018). Some applications for waste catalysts have been reported—for example, applying thermal engineering methods to hazardous spent catalysts to produce value-added products such as ceramics (Sun et al., 2001; Liang et al., 2011; Mymrin et al., 2017; Ramezani et al., 2017), high strength bricks (Sun, 2003), and cement (Furimsky, 1996; Marafi and Stanislaus, 2003). This is considered an attractive option from environmental and economic points of view.

Excess energy consumption, however, is an important feature for thermal treatment processes, which limits its further large-scale application. It is well known that waste SCR catalysts contain a large amount of refractory TiO_2 (more than 70% in weight), which requires even more energy. For the purpose of reducing the energy required during thermal treatment, lowering the melting point by using proper additives is an option. Different oxides play different roles in the melting process (Takaoka et al., 1997; Cheng et al., 2002; Wang et al., 2017). SiO_2 acts as the main network forming oxide of silicate structures. CaO , Na_2O , K_2O , and Fe_2O_3 are commonly used as oxides for glass forming, melting, and matrix modifying, which can change glass properties, and the high content of basic oxide may lead to matrix stability problems. Al_2O_3 is an intermediate substituted for a network former and has the same function as a network modifier. Kuo et al. (2003) pointed out that the addition of SiO_2 enhances the formation of interconnected glass network structures and helps to improve the chemical stability of heavy metals in molten slag. Li et al. (2007) and Cheng et al. (2013) found that CaO contributes to vitrification and improves the heavy metal solidification of slag, thus reducing the melting point of fly ash and making the melting treatment easier. Yang et al. (2009) added Fe_2O_3 and CaO into MSWI fly ash to form a SiO_2 - CaO - Al_2O_3 - Fe_2O_3 quaternary phase system, and significantly reduced the melting temperature from 1500 °C to 1200 °C. Shi et al. (2017) showed that Fe_2O_3 and TiO_2 act as nucleating agents to promote melting and the crystallization of CaO - Al_2O_3 - SiO_2 glass, thereby reducing crystallization temperatures. Li et al. (2016) studied the effect of Al_2O_3 addition on the phase transformation of Ti-bearing blast furnace slag with different basicities. The results showed that an increase of Al_2O_3 content prompted crystallization of

the slags with basicities of 0.60 and 0.75, whereas it suppressed the crystallization with a basicity of 0.95.

The melting characteristics of solid waste during thermal treatment are a significant issue that needs to be studied in depth. However, to the best of our knowledge, many studies focus on the melting characteristics of MSWI fly ash, but seldom on the waste SCR catalyst. Our research group has conducted a preliminary exploration of the feasibility of applying a thermal melting treatment to a waste SCR catalyst in previous work (Zhou et al., 2017), and found that the heavy metals in waste SCR catalysts can be effectively immobilized by thermal melting treatment. However, the melting characteristics of waste SCR catalysts with additives were not described. In this study, further research on the harmless treatment of waste SCR catalysts was carried out. An in-situ investigation of the effects of additives on melting properties and the mineral phase transformation of waste SCR catalysts was carried out through heating stage microscopy, thermogravimetric analysis/differential scanning calorimetry (TG/DSC) thermal analysis, X-ray diffraction (XRD) analysis, and FactSage simulation, and an optimal additive group was determined. In addition, the heavy metal leaching characteristics of waste SCR catalysts after melting treatments were tested by inductively coupled plasma-atomic emission spectrometry (ICP-AES) analysis to evaluate the immobilization of heavy metals.

2 Materials and methods

2.1 Materials

The waste SCR catalyst was collected from the flue-gas denitration system of a coal-fired power plant in China, as shown in Fig. 1. The waste SCR catalyst was crushed and sieved within 0.074 mm, and then analyzed using a scanning electron microscope-energy dispersive spectrometer (SEM-EDS), ICP-AES, X-ray fluorescence (XRF), and heavy metal leaching tests. The chemical composition and heavy metal leaching concentration of the waste SCR catalyst are presented in Tables 1–3.

The XRF results indicate that the waste SCR catalyst can be classified as a vanadium-titanium-based catalyst, whose main composition is TiO_2 (72.341% in weight). The presence of SiO_2 , Al_2O_3 , and CaO is mainly caused by the fly ash adhered on

the surface of the waste SCR catalyst, which is one reason for the deactivation of the SCR catalyst. Because of the relatively low accuracy of XRF for trace elements such as As, Se, Zr, Pb, Zn, and Sr, the waste SCR catalyst was digested and diluted by deionized water to 100 mL. Then, the contents of such elements in the digestion solution were determined by ICP-AES so that the mass fractions of each in the waste SCR catalyst were obtained. The ICP-AES results are relatively lower than those from XRF, mainly because of the difference between elements and oxides, and the accuracies of the different detection methods. The leaching concentration of V in the raw sample is much higher than the standard limit, and As, Pb, and Se have a relatively high level with the potential risk of leaching due to the complex environmental conditions of waste SCR catalysts in the long run.

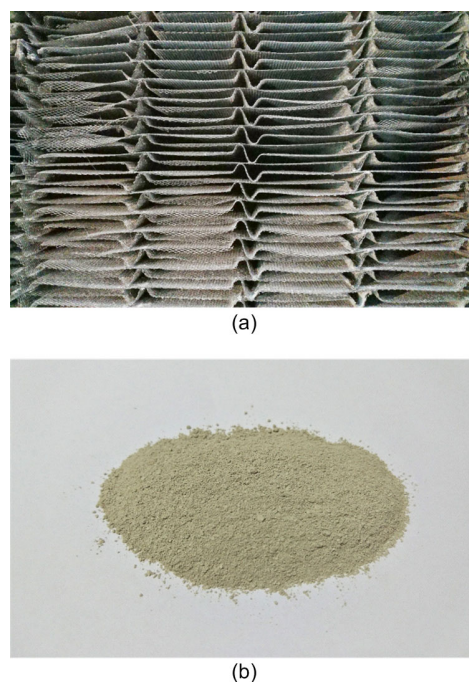


Fig. 1 Plate-type (a) and pulverized (b) waste SCR catalysts

The energy cost for the melting treatment of waste SCR catalysts is unfeasibly high because of high melting temperatures. In order to promote the melting of the waste SCR catalyst, several groups of additives were used to investigate whether additives contribute to the melting behavior of the catalyst and which group of additives shows optimal melting behavior. Considering the role that each oxide plays during the melting process, four oxides were selected

Table 1 Chemical composition of the waste SCR catalyst

Composition	Mass fraction (%)
TiO ₂	72.341
SiO ₂	10.882
Al ₂ O ₃	7.165
V ₂ O ₅	3.902
SO ₃	2.012
MoO ₃	1.546
P ₂ O ₅	1.331
CaO	0.264
Nb ₂ O ₅	0.160
K ₂ O	0.118
Na ₂ O	0.085
MgO	0.071
As ₂ O ₃	0.054
SeO ₂	0.034
ZrO ₂	0.021
PbO	0.0069
ZnO	0.0042
SrO	0.0034

Table 2 ICP-AES results of the waste SCR catalyst

Element	Mass fraction (%)
As	0.015194
Se	0.001237
Zr	0.000996
Pb	0.000278
Zn	0.000186
Sr	0.011697

Table 3 Toxicity leaching results of the waste SCR catalyst

Element	Toxicity leaching (mg/L)	
	Raw sample	Regulatory standard limit
V	10.648	0.20*
As	1.054	5
Pb	0.195	5
Se	0.347	1

* Defined by universal treatment standard (UTS) instead of GB 5085.3-2007 (MEE, 2007a)

as additives, namely CaO, Fe₂O₃, SiO₂, and Al₂O₃ (at analytical reagent grade). SiO₂ can act as a flux and form eutectoids with other oxides, lowering the melting temperature of the samples. Fe₂O₃ and CaO can be added together to promote crystallization behavior and the formation of eutectic low melting points. However, the fluxing effect of CaO is related to its content and to the SiO₂/Al₂O₃ ratio. Al₂O₃ is added to adjust the SiO₂/Al₂O₃ ratio, though it may

increase the melting temperature. The samples were divided into A, B, and C groups according to different additives. The proportions of additives were set based on the phase diagrams shown in Fig. 2, which came from PhaseDiagram-Web and Phase Equilibria Diagram Database 3.1.0 (Zhou et al., 2017). According to the low-melting-point areas in phase diagrams, the optimal proportions of additives can be determined so that their melting behavior is optimized and, consequently, the overall melting performance of the mixture is improved. The proportions of waste catalyst were set as 10%, 50%, and 90% respectively in each group in order to highlight the effects of the additives. All the samples were weighed (10 g), and homogeneously mixed according to Table 4 for subsequent experiments. The main chemical compositions of samples with additives are listed in Table 5.

2.2 Heating stage microscope

The morphology and size change of samples during melting were monitored in-situ by heating stage microscope. As shown in Fig. 3, the heating stage microscope consists primarily of six parts: the heating unit, microscope, charge coupled device (CCD) camera, cooling water, temperature controller, and online computer system. The sample particles were placed in the holder of the heating unit at room temperature under an air atmosphere, and then first heated to 1000 °C at the rate of 40 °C/min, and then to the highest temperature of 1400 °C with a lower heating rate of 25 °C/min for the purpose of protecting the heating stage from damage under high temperature. The samples were held at 1400 °C for 5 min and then cooled down at 40 °C/min to room temperature. The morphology changes of the samples during the heating process were observed by light microscope and recorded by an online computer system with image analysis software in real time. The magnification used in this study was 100 times.

The dimensional changes of the samples were quantified by the image processing software Image J 1.52a, and the area shrinkage was calculated by

$$\text{Area shrinkage} = \frac{A_0 - A}{A_0} \times 100\%, \quad (1)$$

where A_0 and A are the initial area of the samples and the area of the samples at a specific temperature, respectively.

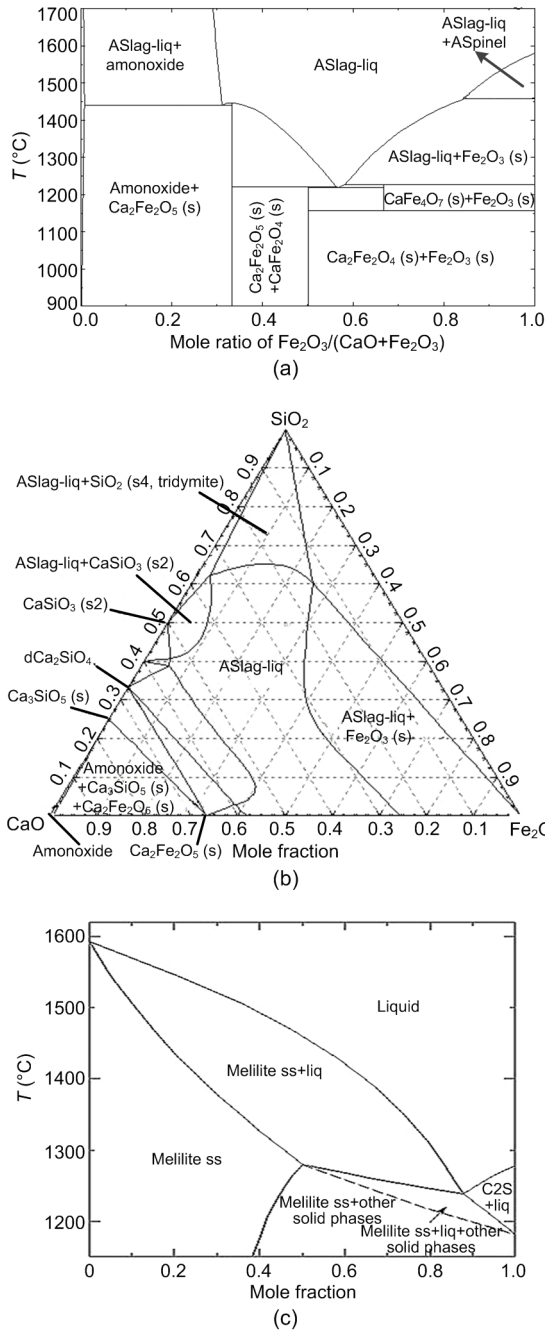


Fig. 2 Multicomponent phase diagrams based on the additive composition (a) CaO-Fe₂O₃; (b) CaO-Fe₂O₃-SiO₂; (c) CaO-Fe₂O₃-SiO₂-Al₂O₃. C2S: 2CaO·SiO₂; ss: solid solution

2.3 TG/DSC test

The melting characteristics of the nine samples and the pure waste SCR catalyst without additives were investigated by a TG/DSC test using a simultaneous thermal analyzer (4, TG/DSC 3+) with a

temperature accuracy of ±0.5 °C. About 10 mg of sample powders were placed in a Pt crucible and heated at 25 °C/min from room temperature to a final temperature of 1400 °C under a continuous air flow of 50 mL/min. The TG and DSC curves, which provided quantitative information about the mass variations

Table 4 Sample compounds with three groups of additives

Sample	Mass fraction (%)				
	Catalyst	CaO	Fe ₂ O ₃	SiO ₂	Al ₂ O ₃
A1	10.00	18.00	72.00	–	–
A2	50.00	10.00	40.00	–	–
A3	90.00	2.00	8.00	–	–
B1	10.00	24.30	54.00	11.70	–
B2	50.00	13.50	30.00	6.50	–
B3	90.00	2.70	6.00	1.30	–
C1	10.00	11.70	70.20	5.94	2.16
C2	50.00	6.50	39.00	3.30	1.20
C3	90.00	1.30	7.80	0.66	0.24

Table 5 Chemical composition of the samples with additives

Sample	Mass fraction (%)				
	TiO ₂	CaO	Fe ₂ O ₃	SiO ₂	Al ₂ O ₃
A1	7.234	18.026	72.000	1.088	0.717
A2	36.171	10.132	40.000	5.441	3.583
A3	65.107	2.238	8.000	9.794	6.449
B1	7.234	24.326	54.000	12.788	0.717
B2	36.171	13.632	30.000	11.941	3.583
B3	65.107	2.938	6.000	11.094	6.449
C1	7.234	11.726	70.200	7.028	2.877
C2	36.171	6.632	39.000	8.741	4.783
C3	65.107	1.538	7.800	10.454	6.689

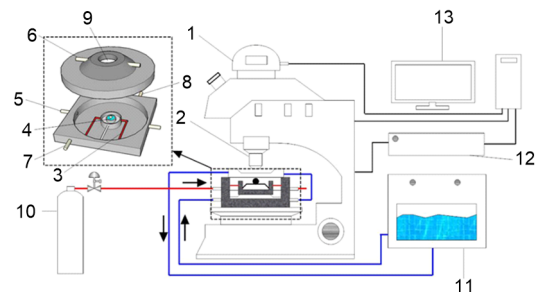


Fig. 3 Schematic diagram of the heating stage microscope 1: digital camera; 2: microscope lens; 3: heating wire; 4: sapphire substrate; 5: water inlet; 6: water outlet; 7: gas inlet; 8: gas outlet; 9: quartz glass; 10: air cylinder; 11: cooling water tank; 12: temperature controller; 13: online computer system

and thermal transformation of the sample as a function of temperature, were recorded in real time for thermal property analysis.

2.4 Thermodynamic equilibrium calculations

The thermodynamic software package FactSage 5.2 was used to calculate the mineral phase transition and the variation of the liquid phase proportion of the waste SCR catalyst with and without additives at high temperature. The waste SCR catalyst was simplified and normalized to the $\text{TiO}_2\text{-SiO}_2\text{-Al}_2\text{O}_3\text{-V}_2\text{O}_5\text{-SO}_3\text{-MoO}_3\text{-P}_2\text{O}_5$ multicomponent system based on its chemical composition presented in Table 1, and corresponding additives were added into the system for each sample. The databases used in the calculation included the FACT 50 compound database and the FToxid solution database. The Norma algorithm in the Equilib module was selected. The calculation temperature range was from 800 °C to 1600 °C, in incremental steps of 20 °C. The calculation was carried out in air atmosphere (21:79 O_2 -to- N_2 volume ratio) at 101 325 Pa, with the excess air ratio set at 1, which is consistent with the experimental data. The calculation results were verified by the XRD analysis for the samples after the melting treatment at different temperatures.

2.5 Leaching toxicity test

In order to evaluate the immobilization of heavy metals after the melting treatment, the toxicity leaching characteristics of the waste SCR catalyst before and after melting were tested according to the standard HJ/T 300-2007 (MEE, 2007b) about extraction procedure for leaching toxicity. The slag used for the leaching toxicity test was obtained by heating a raw sample at 1400 °C for 60 min under air atmosphere in a high-temperature tube furnace. In the leaching procedure, a 2-g sample (raw waste catalyst or catalyst slag) was first finely ground and mixed with 40 mL leachate with a liquid-solid ratio (L/S) of 20:1 (L/kg) in a sealed polyethylene bottle. Then, the bottle was tumbled at 30 r/min using an electric rotary extractor for 18 h at room temperature. Following this, the leachate was filtered and collected to determine the heavy metal concentrations by ICP-AES. In all leaching tests, the leachate was prepared by diluting a 5.7-mL acetic acid and 64.3-mL 1-mol/L NaOH mixed solution with 1 L of deionized water.

3 Results and discussion

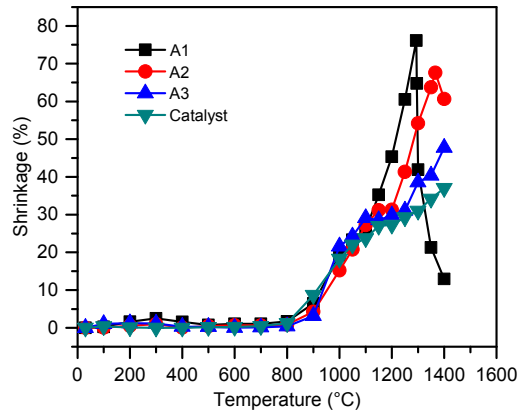
3.1 Effect of additives on area shrinkage

The area shrinkage of samples with different additives as a function of temperature is presented in Fig. 4. Adding additives into a waste SCR catalyst can significantly increase the area shrinkage at high temperature, which verifies that a volume reduction of solid waste can be achieved by thermal melting treatment. When the additive proportion accounts for 50% or 90% (in weight), the area shrinkage of samples for all three groups decreases after reaching the maximum value, indicating that an obvious liquid phase appears and then spreads around the samples as the temperature rises further. This can be explained by the surface tension of the liquid phase formed on the sample surface at high temperatures, which gives the surface a tendency to shrink. Such a phenomenon becomes more significant as the temperature rises. However, the surface tension of the liquid phase decreases with the increase in temperature. When the temperature reaches a certain value, the bead formed by the molten phase breaks and the liquid diffuses around the sample. The slag viscosity also decreases with rising temperature, improving the fluidity of the slag. However, with 10% or no additives added, the area shrinkage of samples increases monotonically with increasing temperature, indicating that there is no liquid phase formed throughout the heating temperature range.

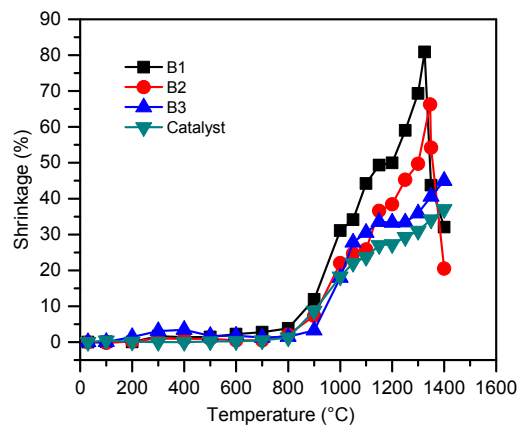
The data results summarized from Fig. 4, namely the maximum area shrinkage ($\text{Shrink}_{\text{max}}$), the temperature when the maximum area shrinkage occurs (T_{max}), and the area shrinkage at the highest temperature of 1400 °C ($\text{Shrink}_{1400^\circ\text{C}}$), are listed in Table 6. For groups A and B, the $\text{Shrink}_{\text{max}}$ of samples increases with the increase of additives, and the T_{max} reverses. For group C, the $\text{Shrink}_{\text{max}}$ of samples with 50% additives is close to that of 90%, which means that the additive composition of group C can achieve high shrinkage under a relatively low additive proportion. Furthermore, the T_{max} of samples in group C is lower than that in groups A and B when adding 90% or 50% additives. For example, for C2, the T_{max} is 1288 °C, while it is 1366 °C and 1346 °C for A2 and B2, respectively. The T_{max} can be used to characterize the melting of samples, and thus the results above

indicate that the additive compositions of group C are more conducive to achieving melting for waste SCR catalysts, meeting the requirements of energy saving

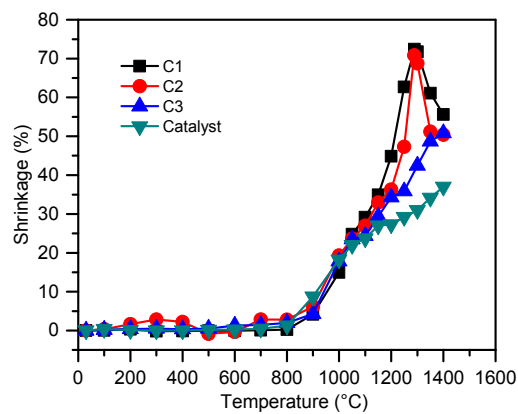
in practical industrial applications. The $\text{Shrink}_{1400^\circ\text{C}}$ also varies with different additives, associated with the molten slag viscosity of samples with different oxidant compositions. A high slag viscosity means poor liquid phase fluidity, and thus the sample area is smaller than that of lower viscosity at 1400°C .



(a)



(b)



(c)

Fig. 4 Area shrinkage of samples with different additives and temperatures

(a) Samples of group A; (b) Samples of group B; (c) Samples of group C

Table 6 $\text{Shrink}_{\text{max}}$, T_{max} , and $\text{Shink}_{1400^\circ\text{C}}$ for all samples

Sample	$\text{Shrink}_{\text{max}}$ (%)	T_{max} ($^\circ\text{C}$)	$\text{Shrink}_{1400^\circ\text{C}}$ (%)
A1	76.11	1293	12.95
A2	67.63	1366	60.62
A3	47.75	1400	47.75
B1	80.85	1325	32.06
B2	66.25	1346	20.48
B3	44.98	1400	44.98
C1	72.43	1289	55.60
C2	70.85	1288	50.39
C3	50.80	1400	50.80
Waste SCR catalyst	37.03	1400	37.03

3.2 Effect of additives on melting temperature

The DSC curve reflects the physical and chemical changes of samples because of endothermic and exothermic reactions during heating. The melting process is an endothermic reaction, corresponding to an endothermic peak on the DSC curve (Li et al., 2007; Liu et al., 2012; Zhang et al., 2017).

Fig. 5 shows the DSC curves of samples in different groups with the same additive level in the temperature range of $1000\text{--}1400^\circ\text{C}$. For samples with 90% and 50% (in weight) of additives, there are obvious endothermic peaks in DSC curves when temperatures are higher than 1100°C , and some even have more than one endothermic peak, which means that distinct and continuous melting reactions occurred at high temperatures. However, no significant melting occurred in samples with 10% additives because of the high mass fraction (90%) of waste SCR catalysts (mainly TiO_2 with a high melting point).

The temperatures at the endothermic peaks (T_{peak}) can be used to characterize the melting temperatures of samples, which are listed in Table 7. The results show that with 90% additives, the first T_{peak} of groups A, B, and C are 1166°C , 1210°C , and 1139°C , while those for 50% additives are 1154°C , 1219°C , and 1139°C , respectively.

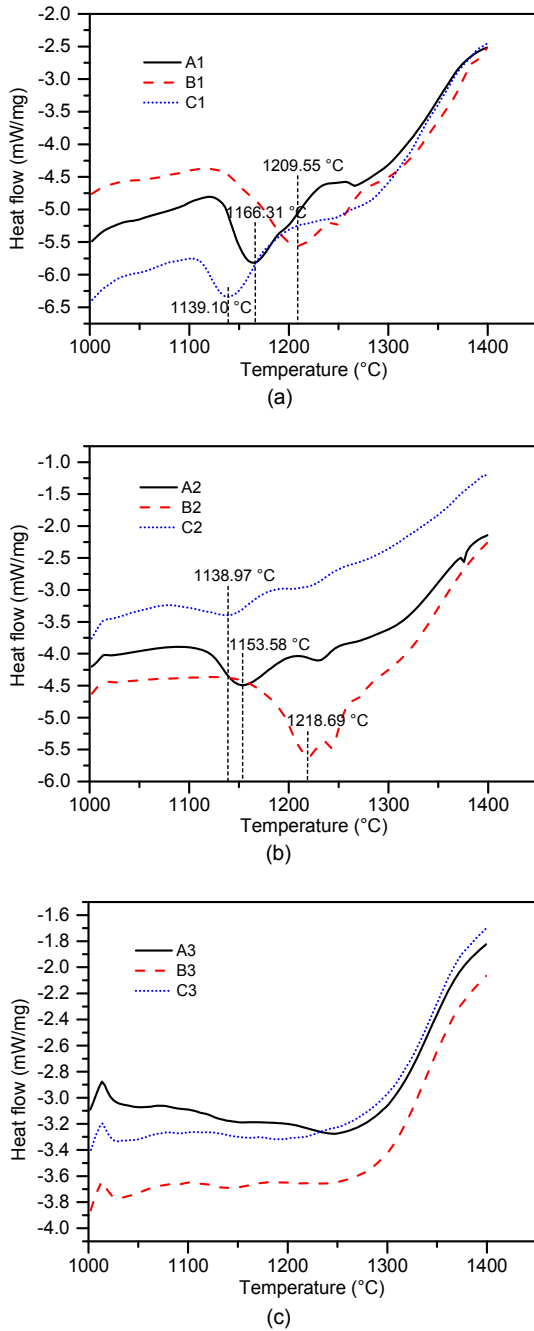


Fig. 5 DSC curves of samples in different additive groups (a) 90% additives; (b) 50% additives; (c) 10% additives

The melting temperatures of samples in each group follow an ascending sequence of group C < group A < group B, which means that the additive formula of group C (Fe_2O_3 , CaO , SiO_2 , and Al_2O_3) achieves the optimal fluxing behavior, followed by that of group A (Fe_2O_3 and CaO), while the additive formula of group B (Fe_2O_3 , CaO , and SiO_2) shows the

worst fluxing behavior. This analysis corresponds well with the area shrinkage results.

The melting point is related to the oxide components of the samples. Previous studies have shown that acidic oxides tend to form polymers, which increase the melting point, while basic oxides inhibit the formation of polymers and thus lower the melting point (Gupta et al., 1998). Not only is the melting point controlled by a certain oxide compound, but the interaction between different oxide compounds also has effect on it. The A/B ratio is thus defined as an indicator of melting characteristics, which is the mass ratio of acidic oxides to basic oxides of samples (Zhang et al., 2017).

A/B ratio =

$$\frac{\text{Mass of } (\text{SiO}_2 + \text{Al}_2\text{O}_3 + \text{TiO}_2)}{\text{Mass of } (\text{CaO} + \text{MgO} + \text{Fe}_2\text{O}_3 + \text{Na}_2\text{O} + \text{K}_2\text{O} + \text{SO}_3)} \quad (2)$$

Table 7 Endothermic peak (T_{peak}), A/B ratio, and mass ratio of SiO_2 to Al_2O_3 (Si/Al) of all samples

Sample	T_{peak} (°C)	A/B ratio	Si/Al
A1	1166	0.10	1.52
A2	1154	0.88	1.52
A3	—	6.75	1.52
B1	1210	0.26	3.15
B2	1219	1.16	2.54
B3	—	16.55	1.70
C1	1139	0.21	1.80
C2	1139	1.06	1.70
C3	—	7.22	1.56
Waste SCR catalyst	—	35.45	1.52

According to Table 7, the raw waste SCR catalyst has a highest A/B ratio of 35.45, and after adding a certain proportion of additives, A/B ratio decreases significantly. It has been shown that the melting point of coal ashes decreases as A/B ratio decreases (Zhang et al., 2017). Accordingly, the melting point of waste SCR catalyst decreases with additives added. For the samples in group B, A/B ratio is much higher than in groups A and C, which can explain the worse fluxing effect of group B. However, the A/B ratio of samples in group C is slightly higher than in group A, which is inconsistent with the DSC analysis—the results of which showed that the T_{peak} of group C is lower than that of group A, indicating that the melting behavior

of samples is not only controlled by the A/B ratio, which only represents the general trend of the melting point. The mass ratio of SiO_2 to Al_2O_3 is another important factor affecting the melting behavior of the samples, especially when A/B ratios are close to each other. At a relatively low level of Si/Al (<1.5), melting temperature decreases significantly as Si/Al grows (Liu et al., 2013; Li et al., 2017), while at a higher level of Si/Al, melting temperature increases (Song et al., 2010; Li et al., 2017; Yan et al., 2017) or remains stable (Liu et al., 2013; Li et al., 2017; Yan et al., 2017) with increasing Si/Al. As shown in Table 7, the Si/Al of samples in group C is slightly higher than that in group A when the Si/Al of samples in these two groups are all at a low level, which verifies that the melting temperature of samples in group C is lower than that of group A.

Melting temperature is a complex parameter controlled by oxide compositions and their interaction during the heating process. Moreover, the mineral phase formed by the reaction of oxide compositions during the melting process will further affect the melting behavior, which will be discussed in the next section.

3.3 Mineral phase transformation

Melting behaviors are mainly controlled by the thermodynamics and kinetics of mineral phase transitions at high temperatures (Jak, 2002). The Equilib module of FactSage 5.2 was used to predict the mineral phase transformation and liquid phase generation of the waste SCR catalysts with 50% (in weight) additives between 800 and 1600 °C. The calculation results were also verified by an XRD analysis of the samples after a melting treatment at 1000, 1200, and 1400 °C. The FactSage calculation results and XRD patterns are depicted in Figs. 6 and 7, respectively.

For A2, the mineral phases formed at high temperature are mainly pseudobrookite (Fe_2TiO_5), perovskite-b (CaTiO_3), anorthite ($\text{CaAl}_2\text{Si}_2\text{O}_8$), and little sphene (CaSiTiO_5), of which Fe_2TiO_5 accounts for 60.01% (in weight). In the FactSage calculation, the initial melting temperature, T_{IM} , is defined as the temperature at which the first liquid forms. As shown in Fig. 6a, the T_{IM} of A2 is 1223 °C, and with the temperature rising further, the liquid phase proportion increases rapidly with the decrease of mineral phase compounds. When the temperature reaches 1320 °C,

the liquid phase proportion is stable at 92%. As described before, the temperature at which the maximum area shrinkage occurs, T_{max} , is 1366 °C, which deviates significantly from the FactSage results. There are two main reasons that can explain this: (1) the FactSage simulation is performed based on thermodynamic equilibrium rather than on kinetics and mass transfer, which is different from the actual heating process by the heating stage microscope; (2)

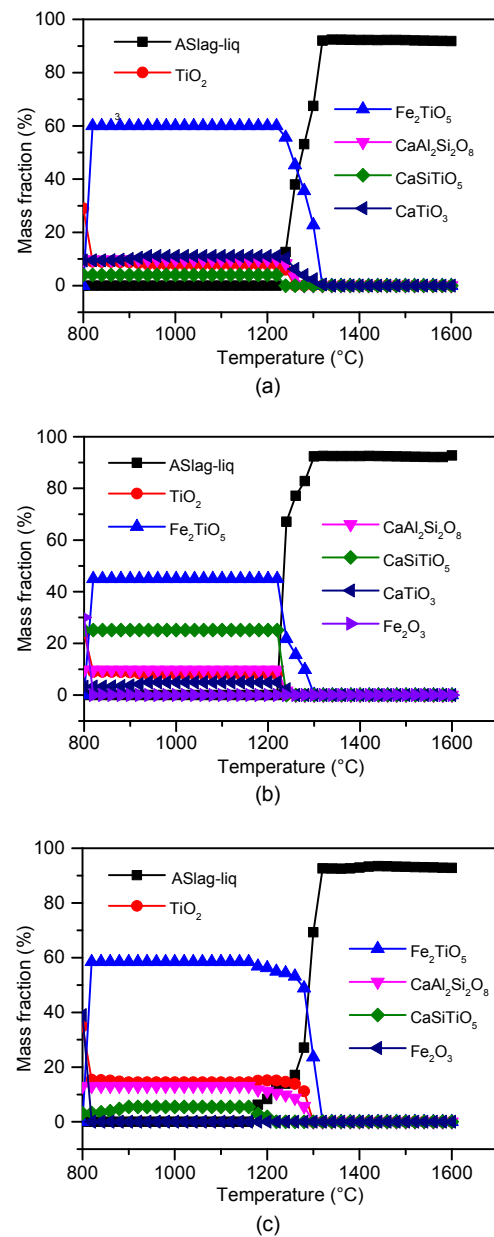


Fig. 6 Mineral transformation behavior of waste SCR catalyst with 50% additives (FactSage calculation results): (a) A2; (b) B2; (c) C2

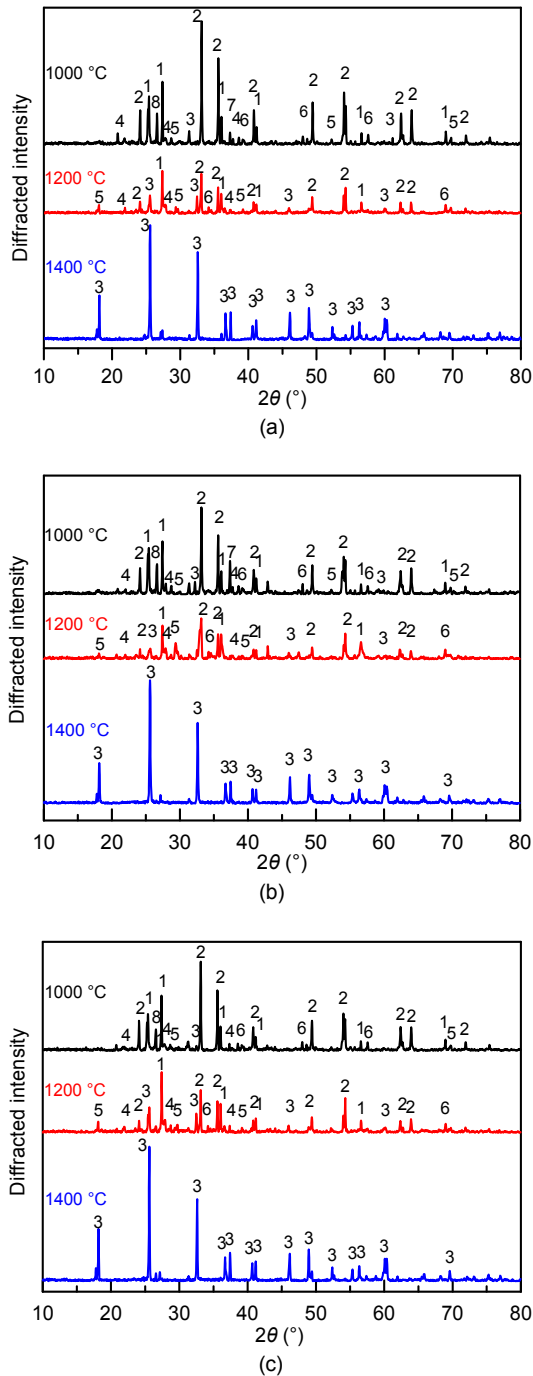


Fig. 7 XRD patterns of the waste SCR catalyst with 50% additives: (a) A2; (b) B2; (c) C2

1: TiO_2 ; 2: Fe_2O_3 ; 3: Fe_2TiO_5 ; 4: $\text{CaAl}_2\text{Si}_2\text{O}_8$; 5: CaSiTiO_5 ; 6: CaTiO_3 ; 7: CaO ; 8: SiO_2

the liquid phase was first generated inside the samples during the shrinkage process, which confirmed that the actual T_{max} is higher than that from calculation (1320 °C).

Compared to A2, Fe_2TiO_5 generated in B2 decreases to 45.01%; CaSiTiO_5 , $\text{CaAl}_2\text{Si}_2\text{O}_8$, and a small amount of CaTiO_3 are also formed at high temperature. The decrease of Fe_2TiO_5 is mainly due to the lower Fe_2O_3 content in B2 than that in A2. The T_{IM} of B2 calculated by FactSage is also 1223 °C, and then the liquid phase proportion increases sharply with increasing temperature and is finally stable at 92% after 1300 °C.

For C2, there are 58.51% Fe_2TiO_5 , 13.05% $\text{CaAl}_2\text{Si}_2\text{O}_8$, and a little CaSiTiO_5 , formed at high temperature, but no CaTiO_3 . What is more, the T_{IM} of C2 decreases to 1169 °C, and the liquid phase proportion initially rises slowly as the temperature increases, then goes up sharply after 1280 °C and remains stable at 92% when the temperature reaches 1320 °C. The decrease of T_{IM} can be explained by the formation of more anorthite ($\text{CaAl}_2\text{Si}_2\text{O}_8$) due to different additives (increases from 9.78% of A2 and B2 to 13.05% of C2), which can easily produce low-melting eutectics with other mineral phases and thus lower melting temperatures of waste SCR catalysts (Qiu et al., 1999; Liu et al., 2013).

With different additives, the T_{IM} decreases from 1223 °C of A2 and B2 to 1169 °C of C2. Therefore, the additive formula of C2 can significantly reduce the melting point of the waste SCR catalyst compared to A2 and B2. Despite the fact that the results obtained by the FactSage calculation deviated from the heating stage experiment, the comparison of results between different samples is consistent; that is, C2 is better than A2 and B2 in terms of lowering the melting point of the waste SCR catalyst.

As discussed above, there is no obvious difference but there are diverse relative proportions between the mineral phases generated at high temperature for A2, B2, and C2, which is consistent with the results of the XRD analysis where similar patterns are obtained for A2, B2, and C2 treated at the same temperature. At 1100 °C, the main crystal phases of the treated samples are Fe_2O_3 and TiO_2 , with little SiO_2 and CaO . Other phases such as Fe_2TiO_5 , CaSiTiO_5 , $\text{CaAl}_2\text{Si}_2\text{O}_8$, and CaTiO_3 are also generated, though at small amounts. With the temperature increasing to 1200 °C, the peaks of Fe_2O_3 and TiO_2 decrease gradually, reacting with each other to form Fe_2TiO_5 ; as does the peak of SiO_2 , which indicates mineral phase transformation or SiO_2 melting

occurred. The resulting dense vitreous silicate plays an important role in the fixation of heavy metals. Other peaks decline as well because the content of the crystal phase decreased with the formation of the liquid phase. At the highest temperature of 1400 °C, only Fe_2TiO_5 is detected in the slag, which indicates that other crystal phases are melted at high temperatures. With the temperature rising from 1000 °C to 1400 °C, the peak values of each phase gradually decline. The main reason for this is that increasing temperature promotes sample melting. The sample first forms low-melting eutectics, and such amorphous vitreous silicate can encapsulate solid phases hard to melt, promoting the overall melting of the waste SCR catalyst.

Based on the mineral phase analysis results, the melting mechanism of waste SCR catalysts with additives can be described as follows: after adding additives, the liquid adhesive phase calcium ferrite (CaFe_2O_4 , CF) with a low melting point of 1478 K (Yang et al., 2018) and the mineral phases such as $\text{CaAl}_2\text{Si}_2\text{O}_8$, which have the tendency to form low-temperature eutectic mixtures, are initially generated. The former liquid adhesive phase flows, wets, and spreads to the surfaces of TiO_2 solid particles, and leads to the dissolving of TiO_2 . According to the thermodynamic principle of mineral phase reactions (Yang et al., 2018), the reactions occurring with TiO_2 are as follows: $\text{CF} + \text{TiO}_2 \rightarrow \text{CaTiO}_3 + \text{Fe}_2\text{O}_3$, $\text{Fe}_2\text{O}_3 + \text{TiO}_2 \rightarrow \text{Fe}_2\text{TiO}_5$. The later mineral phases, such as $\text{CaAl}_2\text{Si}_2\text{O}_8$, form low-temperature eutectics, which then further encapsulate TiO_2 and promote the melting of the waste SCR catalyst.

3.4 Analysis of melting characteristics

The optimal sample C2 was used as a representative for the analysis of melting characteristics. TG/DSC curves, area shrinkage curves, and FactSage calculation data are combined to analyze mass loss, heat loss, and mineral phase transition during heating, thus demonstrating the complex physical and chemical processes, as well as comprehensive melting characteristics.

As shown in Fig. 8, the heating process of the sample can be divided into three stages according to TG/DSC curves and the area shrinkage of sample with temperature, including the solid reaction stage, the sintering stage, and the primary melting stage.

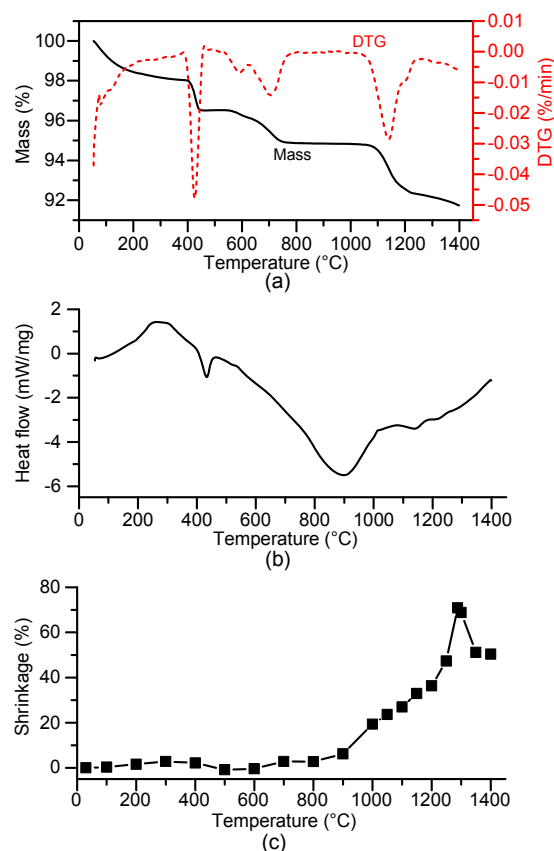


Fig. 8 TG/DSC curves (a), DSC curve (b), and the change of area shrinkage with temperature (c) of sample C2

Stage I (from room temperature to 800 °C): No obvious shrinkage but continuous weight loss of the sample occurs below 800 °C, indicating that there are some mineral phase reactions occurring between solid particles of the waste catalyst with additives in stage I. Thus, it is called the solid reaction stage. As shown in Fig. 8a, the maximum weight loss of C2 below 200 °C is 1.57%, which is mainly due to the evaporation of free water in the sample. Two continuous weight losses are observed at the temperature ranges of 400–500 °C and 600–700 °C, with a maximum weight loss of 2.55%, which is mainly caused by the removal of crystal water in the sample as well as the decomposition of compounds with a low decomposition temperature such as CaCO_3 and $\text{Ca}(\text{OH})_2$. Meanwhile, there is an endothermic peak for samples in 400–500 °C, from which it can be inferred that the polycrystalline transformation happens within crystals in the sample, such as the polymorph transformation between brookite, anatase, and/or rutile (Zhu et al., 2005; Kandiel et al., 2013).

Stage II (from 800 °C to the temperature of reaching the maximum area shrinkage T_{\max}): This stage is identified as the sintering stage, where the preliminary melted phase forms and the area of samples begins to decrease. It can be explained by solid particles congregating with each other and the initial melted phase flowing into open pores (Yan et al., 2016). It is noteworthy that there exists a broad endothermic peak in 800–1000 °C without mass loss, which may be caused by the mineral phase transition under this broad temperature range. Obvious weight loss happens between 1050 and 1200 °C with a maximum weight loss of 3.05%. The weight loss is mainly caused by the decomposition of mineral crystals. Finally, there exists a weak endothermic peak in 1100–1200 °C, which indicates that the solid phase is no longer stable and melting occurs in stage II. This fits well with the T_{IM} of 1169 °C calculated by FactSage, and the area shrinkage in stage II increases from 23.67% to 36.31% correspondingly.

Stage III (from T_{\max} to 1400 °C): The area shrinkage of C2 reaches a maximum value of 70.85% at the sintering stage—the area minimum. As temperature further increases, the sample area increases significantly. The main reason is that the sample collapses at higher temperatures, and the liquid phase increases rapidly due to severe melting, then the liquid phase flows around and hence contributes to the expanding of the sample area (Yan et al., 2016). Most minerals of the sample melt in this stage; thus, stage III is characterized as the primary melting stage. At stage III, the heat flux of the reaction continues to increase, and the weight is slightly reduced. This is owing to the decomposition of residual mineral phase crystals.

3.5 Leaching characteristics of the waste SCR catalyst with additives

As shown above, the waste SCR catalyst with additives of 39.00% (in weight) Fe_2O_3 , 6.50% CaO , 3.30% SiO_2 , and 1.20% Al_2O_3 (C2) achieves the optimal fluxing behavior. In order to examine the heavy metal immobilization of C2 by melting treatment, toxicity leaching experiments were carried out, and the results were listed in Table 8. There is no clear standard limit for V in the Chinese regulatory standard GB 5085.3-2007 (MEE, 2007a). However, the UTS specifies the hazardous waste landfill entry criteria,

which stipulate that the leaching concentration limit for heavy metal V is 0.20 mg/L. As shown in Table 8, the leaching concentration of V in the raw sample was much higher than the standard limit of UTS before the thermal melting treatment. Although the leaching concentrations of other heavy metals, such as As, Pb, and Se, met the standard regulation requirement, they were still at a relatively high level with the potential risk of leaching due to the complex environmental conditions of waste SCR catalysts in the long term. After the melting treatment at 1400 °C, the leaching concentrations of all heavy metals were significantly reduced and were far below the standard limits. As previously analyzed, the initial melting temperature of sample C2 decreased significantly with the addition of optimal additives. As a result, an intense melting reaction occurs at 1400 °C and a dense vitrified matrix structure was formed, which contributes to immobilizing the heavy metals into the silicate glass framework to replace anterior metal or nonmetal ions, and enclosing in the glass slag system via strong bond energy (Cheng et al., 2002; Lin et al., 2009; Yang et al., 2009; Zhang et al., 2014).

Table 8 Toxicity leaching results of raw sample and molten slag of C2

Element	Toxicity leaching (mg/L)		
	Raw sample	Molten slag	Regulatory standard limit
V	10.648	0.178	0.20*
As	1.054	0.025	5
Pb	0.195	0.048	5
Se	0.347	0.003	1

* Defined by UTS instead of GB 5085.3-2007 (MEE, 2007a)

4 Conclusions

The effects of additives on melting characteristics of waste SCR catalysts were in-situ investigated to provide valuable information and an optimal additive formula for the thermal melting treatment of a waste SCR catalyst. The conclusions obtained are as follows:

1. The waste SCR catalyst is a TiO_2 -based oxide mixture with a high melting point which can be effectively reduced by adding proper additives so that the efficiency of the thermal melting treatment can be improved.

2. The fluxing behavior of the additives is characterized by the melting temperature of the samples. The additive formula of C2, namely 39.00% (in weight) Fe_2O_3 , 6.50% CaO , 3.30% SiO_2 , and 1.20% Al_2O_3 , gives optimal fluxing behavior, decreasing the initial melting temperature from 1223 °C to 1169 °C.

3. The melting process of samples is divided into three stages: the solid reaction stage, the sintering stage, and the primary melting stage. The reaction mechanism can be depicted as follows: the liquid adhesive phase generated from the waste catalyst flows, wets, and spreads to the surfaces of TiO_2 particles and reacts with them to generate CaTiO_3 and Fe_2TiO_5 . The later mineral phases form low-temperature eutectics, encapsulating TiO_2 and promoting the melting process.

4. Leaching concentrations of heavy metals in samples with additives added after thermal melting treatment were much lower than those of the raw waste catalyst, which demonstrated that a melting treatment with additives has a strong immobilization capacity for heavy metals in waste SCR catalysts.

Contributors

Hao ZHOU designed the research. Yu-jian XING and Jia-nuo XU carried out the experiment and processed the corresponding data. Jia-nuo XU wrote the first draft of the manuscript. Ming-xi ZHOU helped to organize the manuscript. Hao ZHOU and Yu-jian XING revised and edited the final version.

Conflict of interest

Hao ZHOU, Yu-jian XING, Jia-nuo XU, and Ming-xi ZHOU declare that they have no conflict of interest.

References

- Chen JN, Xu SS, Guo SK, 2016. National hazardous wastes catalogue. *Shanghai Building Materials*, 4:1-11 (in Chinese).
- Cheng LC, Wu SH, Huang KL, et al., 2013. Evaluation of effect of reducing additives during vitrification via simulation and experiment. *Journal of the Air & Waste Management Association*, 63(10):1182-1189. <https://doi.org/10.1080/10962247.2013.809389>
- Cheng TW, Chu JP, Tzeng CC, et al., 2002. Treatment and recycling of incinerated ash using thermal plasma technology. *Waste Management*, 22(5):485-490. [https://doi.org/10.1016/S0956-053X\(01\)00043-5](https://doi.org/10.1016/S0956-053X(01)00043-5)
- Choi IH, Kim HR, Moon G, et al., 2018. Spent $\text{V}_2\text{O}_5\text{-WO}_3/\text{TiO}_2$ catalyst processing for valuable metals by soda roasting-water leaching. *Hydrometallurgy*, 175:292-299. <https://doi.org/10.1016/j.hydromet.2017.12.010>
- Furimsky E, 1996. Spent refinery catalysts: environment, safety and utilization. *Catalysis Today*, 30(4):223-286. [https://doi.org/10.1016/0920-5861\(96\)00094-6](https://doi.org/10.1016/0920-5861(96)00094-6)
- Gupta SK, Gupta RP, Bryant GW, et al., 1998. The effect of potassium on the fusibility of coal ashes with high silica and alumina levels. *Fuel*, 77(11):1195-1201. [https://doi.org/10.1016/S0016-2361\(98\)00016-7](https://doi.org/10.1016/S0016-2361(98)00016-7)
- Jak E, 2002. Prediction of coal ash fusion temperatures with the F*A*C*T thermodynamic computer package. *Fuel*, 81(13):1655-1668. [https://doi.org/10.1016/S0016-2361\(02\)00091-1](https://doi.org/10.1016/S0016-2361(02)00091-1)
- Kandiel TA, Robben L, Alkaim A, et al., 2013. Brookite versus anatase TiO_2 photocatalysts: phase transformations and photocatalytic activities. *Photochemical & Photobiological Sciences*, 12(4):602-609. <https://doi.org/10.1039/C2PP25217A>
- Kikuchi R, 2001. Recycling of municipal solid waste for cement production: pilot-scale test for transforming incineration ash of solid waste into cement clinker. *Resources, Conservation and Recycling*, 31(2):137-147. [https://doi.org/10.1016/S0921-3449\(00\)00077-X](https://doi.org/10.1016/S0921-3449(00)00077-X)
- Kuo YM, Lin TC, Tsai PJ, 2003. Effect of SiO_2 on immobilization of metals and encapsulation of a glass network in slag. *Journal of the Air & Waste Management Association*, 53(11):1412-1416. <https://doi.org/10.1080/10473289.2003.10466307>
- Lee JB, Eom YS, Kim JH, et al., 2013. Regeneration of waste SCR catalyst by air lift loop reactor. *Journal of Central South University*, 20(5):1314-1318. <https://doi.org/10.1007/s11771-013-1617-5>
- Li JZ, Wang XY, Wang B, et al., 2017. Effect of silica and alumina on petroleum coke ash fusibility. *Energy & Fuels*, 31(12):13494-13501. <https://doi.org/10.1021/acs.energyfuels.7b02843>
- Li M, Liu B, Wang XR, et al., 2018. A promising approach to recover a spent SCR catalyst: deactivation by arsenic and alkaline metals and catalyst regeneration. *Chemical Engineering Journal*, 342:1-8. <https://doi.org/10.1016/j.cej.2017.12.132>
- Li RD, Wang L, Yang TH, et al., 2007. Investigation of MSWI fly ash melting characteristic by DSC-DTA. *Waste Management*, 27(10):1383-1392. <https://doi.org/10.1016/j.wasman.2006.11.017>
- Li ZM, Li JF, Sun YQ, et al., 2016. Effect of Al_2O_3 addition on the precipitated phase transformation in Ti-bearing blast furnace slags. *Metallurgical and Materials Transactions B*, 47:1390-1399. <https://doi.org/10.1007/s11663-015-0576-7>
- Liang ZY, Yan GY, Zheng LP, et al., 2011. A primary study on preparation of mullite with solid waste. *Advanced Materials Research*, 233-235:1067-1072. <https://doi.org/10.4028/www.scientific.net/AMR.233-235.1067>
- Lin KL, Huang WJ, Chen KC, et al., 2009. Behaviour of heavy metals immobilized by co-melting treatment of sewage sludge ash and municipal solid waste incinerator fly ash. *Waste Management & Research*, 27(7):660-667.

- <https://doi.org/10.1177/0734242X09103826>
- Lindberg D, Molin C, Hupa M, 2015. Thermal treatment of solid residues from WtE units: a review. *Waste Management*, 37:82-94.
<https://doi.org/10.1016/j.wasman.2014.12.009>
- Liu B, He QH, Jiang ZH, et al., 2013. Relationship between coal ash composition and ash fusion temperatures. *Fuel*, 105:293-300.
<https://doi.org/10.1016/j.fuel.2012.06.046>
- Liu GR, Zhan JY, Zheng MH, et al., 2015. Field pilot study on emissions, formations and distributions of PCDD/Fs from cement kiln co-processing fly ash from municipal solid waste incinerations. *Journal of Hazardous Materials*, 299: 471-478.
<https://doi.org/10.1016/j.jhazmat.2015.07.052>
- Liu YY, Wang JJ, Lin X, et al., 2012. Microstructures and thermal properties of municipal solid waste incineration fly ash. *Journal of Central South University*, 19(3):855-862.
<https://doi.org/10.1007/s11771-012-1083-5>
- Marafi M, Stanislaus A, 2003. Options and processes for spent catalyst handling and utilization. *Journal of Hazardous Materials*, 101(2):123-132.
[https://doi.org/10.1016/S0304-3894\(03\)00145-6](https://doi.org/10.1016/S0304-3894(03)00145-6)
- MEE (Ministry of Ecology and Environment of the People's Republic of China), 2007a. Identification Standards for Hazardous Waste—Identification for Extraction Toxicity, GB 5085.3-2007. Standardization Administration of the People's Republic of China (in Chinese).
- MEE (Ministry of Ecology and Environment of the People's Republic of China), 2007b. Solid Waste—Extraction Procedure for Leaching Toxicity—Acetic Acid Buffer Solution Method, HJ/T 300-2007. MEE (in Chinese).
- Min Y, Qin CD, Shi PY, et al., 2017. Effect of municipal solid waste incineration fly ash addition on the iron ore sintering process, mineral phase and metallurgical properties of iron ore sinter. *ISIJ International*, 57(11):1955-1961.
<https://doi.org/10.2355/isijinternational.isijint-2017-310>
- Min Y, Liu CJ, Shi PY, et al., 2018. Effects of the addition of municipal solid waste incineration fly ash on the behavior of polychlorinated dibenzo-p-dioxins and furans in the iron ore sintering process. *Waste Management*, 77:287-293.
<https://doi.org/10.1016/j.wasman.2018.04.011>
- Mymrin V, Pedroso AM, Ponte HA, et al., 2017. Thermal engineering method application for hazardous spent petrochemical catalyst neutralization. *Applied Thermal Engineering*, 110:1428-1436.
<https://doi.org/10.1016/j.applthermaleng.2016.09.077>
- Pan JR, Huang C, Kuo JJ, et al., 2008. Recycling MSWI bottom and fly ash as raw materials for Portland cement. *Waste Management*, 28(7):1113-1118.
<https://doi.org/10.1016/j.wasman.2007.04.009>
- Peng Y, Li JH, Si WZ, et al., 2015. Deactivation and regeneration of a commercial SCR catalyst: comparison with alkali metals and arsenic. *Applied Catalysis B: Environmental*, 168-169:195-202.
<https://doi.org/10.1016/j.apcatb.2014.12.005>
- Qiu JR, Li F, Zheng Y, et al., 1999. The influences of mineral behaviour on blended coal ash fusion characteristics. *Fuel*, 78(8):963-969.
[https://doi.org/10.1016/S0016-2361\(99\)00005-8](https://doi.org/10.1016/S0016-2361(99)00005-8)
- Ramezani A, Emami SM, Nemat S, 2017. Reuse of spent FCC catalyst, waste serpentine and kiln rollers waste for synthesis of cordierite and cordierite-mullite ceramics. *Journal of Hazardous Materials*, 338:177-185.
<https://doi.org/10.1016/j.jhazmat.2017.05.029>
- Rani DA, Gome E, Boccaccini AR, et al., 2008. Plasma treatment of air pollution control residues. *Waste Management*, 28(7):1254-1262.
<https://doi.org/10.1016/j.wasman.2007.06.008>
- Sakai SI, Hiraoka M, 2000. Municipal solid waste incinerator residue recycling by thermal processes. *Waste Management*, 20(2-3):249-258.
[https://doi.org/10.1016/S0956-053X\(99\)00315-3](https://doi.org/10.1016/S0956-053X(99)00315-3)
- Shang XS, Li JR, Yu XW, et al., 2012. Effective regeneration of thermally deactivated commercial V-W-Ti catalysts. *Frontiers of Chemical Science and Engineering*, 6(1): 38-46.
<https://doi.org/10.1007/s11705-011-1167-z>
- Shi J, He F, Ye CQ, et al., 2017. Preparation and characterization of CaO-Al₂O₃-SiO₂ glass-ceramics from molybdenum tailings. *Materials Chemistry and Physics*, 197: 57-64.
<https://doi.org/10.1016/j.matchemphys.2017.05.028>
- Song WJ, Tang LH, Zhu XD, et al., 2010. Effect of coal ash composition on ash fusion temperatures. *Energy & Fuels*, 24(1):182-189.
<https://doi.org/10.1021/ef900537m>
- Sun DD, 2003. Stabilization treatment for reutilization of spent refinery catalyst into value-added product. *Energy Sources*, 25(6):607-615.
<https://doi.org/10.1080/00908310390195679>
- Sun DD, Tay JH, Cheong HK, et al., 2001. Recovery of heavy metals and stabilization of spent hydrotreating catalyst using a glass-ceramic matrix. *Journal of Hazardous Materials*, 87(1-3):213-223.
[https://doi.org/10.1016/S0304-3894\(01\)00279-5](https://doi.org/10.1016/S0304-3894(01)00279-5)
- Takaoka M, Takeda N, Miura S, 1997. The behaviour of heavy metals and phosphorus in an ash melting process. *Water Science and Technology*, 36(11):275-282.
[https://doi.org/10.1016/S0273-1223\(97\)00691-4](https://doi.org/10.1016/S0273-1223(97)00691-4)
- Verbinnen B, Billen P, van Caneghem J, et al., 2017. Recycling of MSWI bottom ash: a review of chemical barriers engineering application and treatment technologies. *Waste and Biomass Valorization*, 8(5):1453-1466.
<https://doi.org/10.1007/s12649-016-9704-0>
- Wang L, Jamro IA, Chen Q, et al., 2016. Immobilization of trace elements in municipal solid waste incinerator (MSWI) fly ash by producing calcium sulphoaluminate cement after carbonation and washing. *Waste Management & Research*, 34(3):184-194.

- <https://doi.org/10.1177/0734242X15617846>
- Wang XT, Jin BS, Xu B, et al., 2017. Melting characteristics during the vitrification of MSW incinerator fly ash by swirling melting treatment. *Journal of Material Cycles and Waste Management*, 19(1):483-495.
<https://doi.org/10.1007/s10163-015-0449-9>
- Wu WC, Tsai TY, Shen YH, 2016. Tungsten recovery from spent SCR catalyst using alkaline leaching and ion exchange. *Minerals*, 6(4):107.
<https://doi.org/10.3390/min6040107>
- Xiao HP, Ru Y, Peng Z, et al., 2018. Destruction and formation of polychlorinated dibenzo-p-dioxins and dibenzofurans during pretreatment and co-processing of municipal solid waste incineration fly ash in a cement kiln. *Chemosphere*, 210:779-788.
<https://doi.org/10.1016/j.chemosphere.2018.07.058>
- Xu SX, Chen T, Li XD, et al., 2018. Behavior of PCDD/Fs, PCBs, CBzs and PAHs during thermal treatment of various fly ash from steel industry. *Aerosol and Air Quality Research*, 18:1008-1018.
<https://doi.org/10.4209/aaqr.2017.11.0514>
- Yan TG, Kong LX, Bai J, et al., 2016. Thermomechanical analysis of coal ash fusion behavior. *Chemical Engineering Science*, 147:74-82.
<https://doi.org/10.1016/j.ces.2016.03.016>
- Yan TG, Bai J, Kong LX, et al., 2017. Effect of SiO₂/Al₂O₃ on fusion behavior of coal ash at high temperature. *Fuel*, 193:275-283.
<https://doi.org/10.1016/j.fuel.2016.12.073>
- Yang JK, Xiao B, Boccaccini AR, 2009. Preparation of low melting temperature glass-ceramics from municipal waste incineration fly ash. *Fuel*, 88(7):1275-1280.
<https://doi.org/10.1016/j.fuel.2009.01.019>
- Yang MR, Lv XW, Wei RR, et al., 2018. Wetting behavior of TiO₂ by calcium ferrite slag at 1523 K. *Metallurgical and Materials Transactions B*, 49(5):2667-2680.
<https://doi.org/10.1007/s11663-018-1360-2>
- You KK, Ma XC, Liu JT, et al., 2012. Characteristic analysis of SCR flue gas denitrification catalyst in power plant. *Advanced Materials Research*, 518-523:2423-2426.
<https://doi.org/10.4028/www.scientific.net/amr.518-523.2423>
- Zhang YK, Ren QQ, Deng HX, et al., 2017. Ash fusion properties and mineral transformation behavior of gasified semichar at high temperature under oxidizing atmosphere. *Energy & Fuels*, 31(12):14228-14236.
<https://doi.org/10.1021/acs.energyfuels.7b02756>
- Zhang ZK, Li AM, Liang XY, 2014. Effects of basicity (CaO/SiO₂) on the behavior of heavy metals from sludge incineration ash by vitrification treatment. *Advanced Materials Research*, 878:284-291.
<https://doi.org/10.4028/www.scientific.net/amr.878.284>
- Zhao ZP, Guo M, Zhang M, 2015. Extraction of molybdenum and vanadium from the spent diesel exhaust catalyst by ammonia leaching method. *Journal of Hazardous Materials*, 286:402-409.
<https://doi.org/10.1016/j.jhazmat.2014.12.063>
- Zheng YJ, Jensen AD, Johnsson JE, 2005. Deactivation of V₂O₅-WO₃-TiO₂ SCR catalyst at a biomass-fired combined heat and power plant. *Applied Catalysis B: Environmental*, 60(3-4):253-264.
<https://doi.org/10.1016/j.apcatb.2005.03.010>
- Zhou H, Guo XT, Zhou MX, 2017. Influence of different additives on harmless melting treatment of waste SCR catalysts. *Journal of Chinese Society of Power Engineering*, 37(12):999-1006 (in Chinese).
- Zhu KR, Zhang MS, Hong JM, et al., 2005. Size effect on phase transition sequence of TiO₂ nanocrystal. *Materials Science and Engineering: A*, 403(1-2):87-93.
<https://doi.org/10.1016/j.msea.2005.04.029>